Dynamic Correlation Under Isochronal Conditions

C. M. Roland and D. Fragiadakis

Abstract Results of various methods of evaluating the dynamic correlation volume in glassforming liquids and polymers are summarized. Most studies indicate that this correlation volume depends only on the α-relaxation time; that is, at state points associated with the same value of τ_α, the extent of the correlation among local motions is equivalent. Nonlinear dielectric spectroscopy was used to measure the third-order susceptibility. Its amplitude, a measure of the dynamic correlation volume, is constant for isochronal state points, which supports the interpretation of the magnitude of the nonlinear susceptibility in terms of dynamic correlation. More broadly, it serves to establish that for non-associated materials, the cooperativity of molecular motions is connected to their timescale.

1 Introduction

Among the many interesting features of glass formation is that it takes place without obvious structural changes on the molecular level. The static structure factor (variance in the density ρ) reflecting short-range correlations is essentially the same above and below the glass transition temperature, T_g [1, 2]. The only apparent effects of vitrification on structure come from changes in volume. For this reason, the glass transition is usually regarded as a dynamic phenomenon. Translational and rotational motions become drastically slower due to their cooperative nature, as molecules cannot move independently. As shown by various experiments [3–7], this has two related consequences: dynamic heterogeneity, referring to the coexistence of fast- and slow-moving molecules, with the mobility variations persisting for times commensurate with (or longer than [8]) the primary (α) relaxation time, τ_α; and dynamic correlation, which refers to the mutual interdependence that extends over some length scale. Molecular dynamics (MD) simulations show that these two properties are correlated for a given material, but not generally (Fig. 1; [9]). Characteristics of the glass transition result from these many-body effects, including the distribution of mobili-

C. M. Roland (✉) · D. Fragiadakis
Naval Research Laboratory, Chemistry Division, Washington, DC 20375-5342, USA
e-mail: mike.roland@nrl.navy.mil

R. Richert (ed.), *Nonlinear Dielectric Spectroscopy*, Advances in Dielectrics
https://doi.org/10.1007/978-3-319-77574-6_8

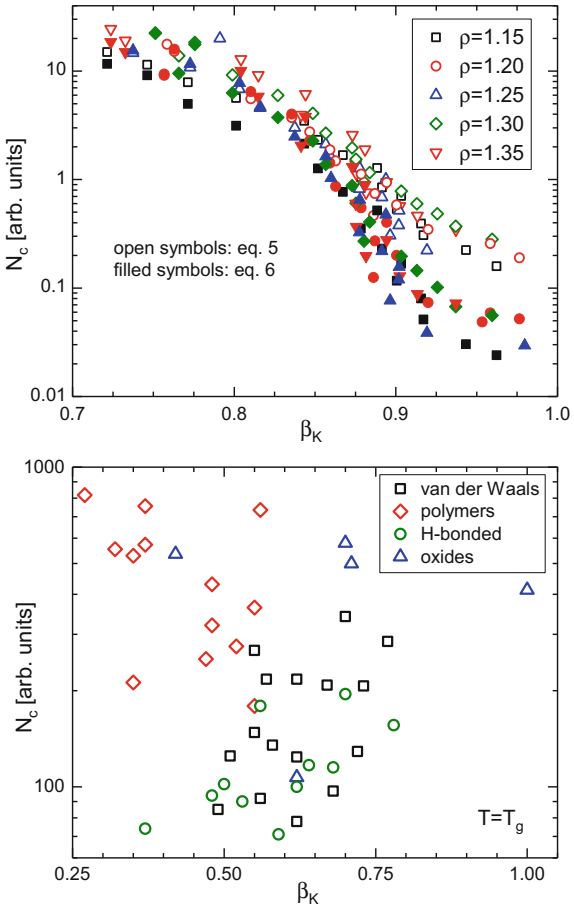

Fig. 1 Comparison of dynamic correlation and the distribution of relaxation times, both reflections of dynamic heterogeneity: (top) MD simulations of the Kob-Andersen binary mixture of Lennard-Jones particles; (bottom) experimental data for different glassforming materials [9]

ties reflected in the breadth of the relaxation dispersion (non-Debye relaxation) and the non-Arrhenius temperature dependence; unsurprisingly, these two properties are connected [10, 11].

Heterogeneous dynamics defines a length scale, ξ, or relatedly the number of dynamically correlated molecules (or polymer segments)

$$N_c \leq \frac{4\pi\rho N_A}{3m}\xi^3 \tag{1}$$

where M is the molecular weight (of the repeat unit for polymers) and N_A is Avogadro's number. Dynamic heterogeneity can be observed directly in colloids [12] and

granular systems [13], although for molecular liquids it is difficult to measure because both spatial and temporal correlations are involved. Nevertheless, such information is a prerequisite for "solving" the glass transition problem. If τ_α is coupled to a dynamic correlation length, theoretical models that address τ_α are making predictions, explicitly or otherwise, for ξ. It is for this reason among others that dynamic correlations are an essential component of theoretical efforts [14–18]. Our purpose herein is to review the available data on the connection, if any, between τ_α and ξ or N_c.

2 Determination of Dynamic Correlation Volume

A variety of methods have been used to estimate ξ or N_c. One approach is confinement of the material to spatial dimensions on the order of ξ. Nanoscale confinement can be imposed in one dimension as in supported or freestanding thin films, in two dimensions, e.g., porous glasses, or three dimensions for nano-sized droplets. It is well established that in the absence of adhesion to the walls [19–21], such geometric confinement of supercooled liquids accelerates their dynamics. One interpretation is that the speeding up of local motions occurs when confinement dimensions are on the order of the cooperative length scale. Experiments along these lines yield estimates of ξ in the range of 2–10 nm; that is, several intermolecular distances, increasing with decreasing temperature [22–26].

Using computer simulations, ξ can be estimated in a similar but more rigorous way using a so-called point-to-set construction [27–31]. Typically, in this method a subset of particles from an equilibrium configuration is frozen, forming an amorphous wall, and ξ is defined as the length over which the effect of the wall on liquid dynamics propagates into the liquid. Alternatively, the particles may be frozen to form geometries of a frozen spherical cavity, a thin film of liquid confined between frozen walls, or a set of randomly pinned particles, thus imposing a confining length scale on the system (size of the cavity, film thickness, and distance between pinned particles, respectively), with ξ determined by the dependence of dynamics on the confining length, mirroring experiments on dynamics in confinement. This method has also been experimentally realized on colloidal glasses for the wall and random pinning geometries [32, 33]. The dynamic length scale obtained in this way generally grows on cooling. For some systems in amorphous wall geometries, however, a nonmonotonic temperature dependence of ξ is observed [30, 31]. It is unclear whether this is an intrinsic property of the liquid related perhaps to change in the shape of cooperative rearranging regions with temperature [30], or an effect arising from particularities of dynamics near a wall [34].

Another method relies on structural length scales that are not imposed externally but already exist within the liquid. Polymer chains provide such a length scale: the end-to-end distance (coil size) with a corresponding timescale, the normal mode relaxation. Using the argument that relaxation times and dynamic length scales are correlated, if two processes have the same relaxation time at a temperature T, at this temperature the spatial extent of the molecular motions corresponding to the

relaxation will be the same. This line of reasoning leads to the supposition that segmental relaxation times and (extrapolated) relaxation times for the normal mode (end-to-end relaxation) of a polymer are equal at state points for which ξ equals the chain coil size [35]. For polypropylene and polyisoprene near T_g, the method yields $N_c \sim 20$, increasing to $N_c > 200$ for temperatures a few degrees below T_g [6, 36, 37].

The above methods of determining dynamic length scales are indirect; Spiess and coworkers pioneered the use of multidimensional ^{13}C solid-state exchange NMR to directly determine the length scale of dynamic heterogeneities [38–40]. Combining two 2-D spin-echo pulse sequences, the experiment measures the fluctuations within the distribution of relaxation rates. Values of ξ in the range 1–4 nm were obtained at temperatures slightly above T_g [38, 39, 41].

Dynamic heterogeneity reflects spontaneous fluctuations about the average dynamics. By relating fluctuations in the entropy to fluctuations of temperature, Donth and coworkers [42, 43] derived a formula for the number of dynamically correlated molecules in terms of the breadth of the calorimetric glass transition temperature

$$N_c = \frac{k_B N_A}{M} \Delta c_p^{-1} \left(\frac{T}{\delta T} \right)^2 \tag{2}$$

In this equation, k_B is the Boltzmann's constant, Δc_p is the isobaric heat capacity change at T_g, and δT is the half-width of the glass transition in temperature units. A slightly different expression is used by Saiter et al. [44]

$$N_c = \frac{k_B N_A}{M} \Delta \left(c_p^{-1} \right) \left(\frac{T}{\delta T} \right)^2 \tag{3}$$

with a different way of taking into account the heat capacity; there is therefore a certain degree of arbitrariness in the values computed by these methods. Assuming a spherical correlation volume, values of ξ at T_g in the range 1–3 nm have been reported [45].

Linear two-time correlation functions describe only the average dynamics and higher order correlation functions, characterizing fluctuations of dynamics about the mean, are used to probe cooperative motions. The multidimensional NMR experiment described above is a four-time correlation method. The spatial extent of dynamic correlations over the timescale t can be quantified more thoroughly through the use of two-time, two-point functions. An example is for the spatial decay of the temporal correlation of the local density [46, 47]

$$C_4(r, t) = \langle \delta\rho(0, 0)\delta\rho(0, t)\delta\rho(r, 0)\delta\rho(r, t) \rangle - \langle \delta\rho(0, 0)\delta\rho(0, t) \rangle \langle \delta\rho(r, 0)\delta\rho(r, t) \rangle \tag{4}$$

where $\delta\rho(r, t)$ is the deviation from the mean density. $C_4(r, t)$ or its Fourier transform, the dynamic susceptibility, can be measured on colloids [12] and granular systems [13]; however, spontaneous fluctuations of molecular liquids are not directly acces-

sible. Berthier and coworkers [42, 48] have shown that the underlying dynamic heterogeneity can be quantified by analyzing induced fluctuations. If the forcing quantity is temperature [49],

$$N_c = \max\left[\frac{N_\mathrm{A}}{M}\frac{k_\mathrm{B}}{\Delta c_p}T^2\left(\chi_T^{\mathrm{NPT}}(t)\right)^2 + \chi_4^{\mathrm{NPH}}(t)\right] \tag{5}$$

The dynamical susceptibility has a maximum as a function of time around $t=\tau_\alpha$, which grows in magnitude on approach to the glass transition. From MD simulations, the contribution of various terms to the dynamic fluctuations can be evaluated, which led to the conclusion that χ_4^{NPH}, representing fluctuations in the isoenthalpic–isobaric ensemble, is negligible at lower temperatures approaching T_g [44, 50]. This enables the number of correlating molecules to be expressed in terms of experimentally accessible quantities [51]

$$N_c \approx \frac{N_\mathrm{A}}{M}\frac{k_\mathrm{B}}{\Delta c_p}T^2\left(\left.\frac{\partial\phi(t)}{\partial T}\right|_p\right)^2 \tag{6}$$

In Eq. (6), $\phi(t)$ is a linear susceptibility, such as the dielectric relaxation function, $\varepsilon(t)$. Figure 1 shows a comparison of N_c from Eqs. (5) and (6); the agreement is good at longer τ_α. Capaccioli et al. [52] used Eq. (6) to analyze data for a large number of liquids, obtaining values of N_c in the range 100–800 at T_g.

Considering other factors such as the density or enthalpy that contribute to dynamic heterogeneity leads to alternatives for Eq. (5), e.g., [44]

$$N_c = \max\left[\frac{N_\mathrm{A}}{M}\frac{k_\mathrm{B}}{\Delta c_V}T^2\left(\chi_T^{\mathrm{NVT}}(t)\right)^2 + \frac{N_\mathrm{A}}{M}k_\mathrm{B}T\kappa_T\rho^3\left(\chi_\rho^{\mathrm{NPT}}(t)\right)^2 + \chi_4^{\mathrm{NVE}}(t)\right] \tag{7}$$

in which Δc_V is the isochoric heat capacity change at T_g, and κ_T is the isothermal compressibility. Assuming fluctuations in the microcanonical (NVE) ensemble are small (MD simulations provide support for $\chi_4^{\mathrm{NVE}}(t)$ becoming smaller with decreasing T [53])

$$N_c \approx \frac{N_\mathrm{A}}{M}\frac{k_\mathrm{B}}{\Delta c_V}T^2\left(\left.\frac{\partial\phi(t)}{\partial T}\right|_V\right)^2 + \frac{N_\mathrm{A}}{M}k_\mathrm{B}T\kappa_T\rho^3\left(\left.\frac{\partial\phi(t)}{\partial\rho}\right|_T\right)^2 \tag{8}$$

The first term on the rhs of Eq. (8) represents fluctuations in the NVT ensemble, with the second term the additional contributions from density fluctuations.

The accuracy of the approximate Eqs. (6) and (8) can be tested by comparing to results using the full Eqs. (5) and (7). As shown in Fig. 1, MD simulations support the underlying assumption that $\chi_4^{\mathrm{NPH}}(t)$ and $\chi_4^{\mathrm{NVE}}(t)$ are negligible. However, N_c for several liquids computed using both Eqs. (6) and (8) differ by as much as 40% (representative results are displayed in Fig. 2) [54]; that is, the difference between two putatively small contributions is an appreciable amount of the total $\chi_4(t)$. This opens to question both absolute values of the correlation volume extracted from the

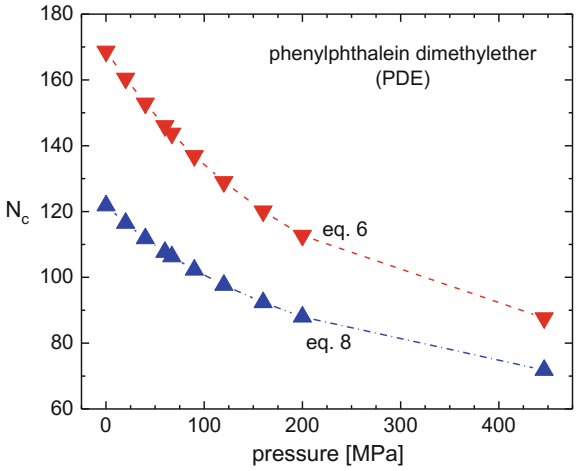

Fig. 2 Number of dynamically correlated molecules calculated assuming contribution from $\chi_4^{\mathrm{NPH}}(t)$ (down triangles) or from $\chi_4^{\mathrm{NVE}}(t)$ (triangles) is negligible. From Ref. [49]

approximate equations, and more significantly, comparisons of N_c made for different state points.

3 Dynamic Correlation Volume at Constant τ_α

If measurements are carried out as a function of temperature and pressure, a determination is possible of any variation of N_c for state points for which τ_α is constant. This approach is not easily applied to confinement experiments, since it is difficult to achieve hydrostatic conditions for materials in pores or very thin films. However, if the confining geometry is used to vary τ_α, a comparison can be made of isochronal N_c at different temperatures and ambient pressures. Koppensteiner et al. [21] confined salol to porous silica, with T_g differing by 8 K for pore sizes = 2.4 and 4.8 nm. They found that N_c from Eq. (6) varied significantly with temperature; however, at temperatures for which the respective τ_α in the different pores were constant, N_c was essentially constant ($\pm$ ~5%). An analogous study of multilayered films of polymethylmethacrylate also found that isochronal N_c was the same for film thicknesses varying from 4 nm up to bulk dimensions (Fig. 3) [55].

Compared to experimental confinement studies, using molecular dynamics simulations, it is much more straightforward to use confinement or a point-to-set construction to determine whether N_c is constant under isochronal conditions. For a molecular liquid in a thin film geometry between confining walls [56], the wall induces a slowing down of dynamics which propagates into the liquid a distance ξ. Although the dependence of dynamics on the distance from the wall was not reported, the spatially averaged dynamics of the film was found to be constant at several different state points with the same bulk τ_α, suggesting that ξ defined in this way must also be constant.

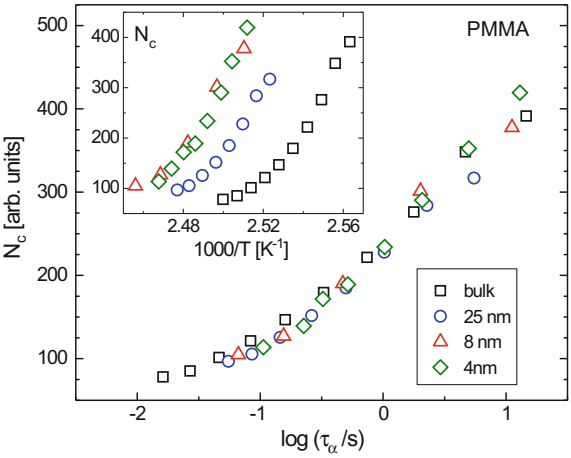

Fig. 3 Number of dynamically correlated segments for polymethylmethacrylate coextruded multilayers. Confinement alters the segmental relaxation time (inset), but N_c from Eq. (6) remains a function of τ_α. From Ref. [50]

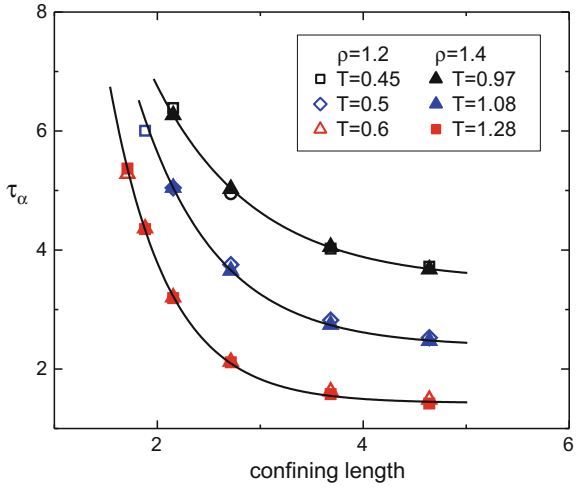

Fig. 4 Relaxation time as a function of confining length $L = c^{1/3}$ of Kob-Andersen Lennard-Jones mixture, with fraction c of pinned particles, simulated at the indicated state points. Each pair of state points is chosen to have the same bulk (unpinned) τ_α

Dynamic correlations can also be investigated using random pinning: pinning a fraction c of atoms or molecules is essentially equivalent to imposing a "confining length scale" equal to the distance between pinned particles $L \sim c^{1/3}$. With increasing pinning fraction, as the confining length scale impinges on ξ, dynamic correlations cause the dynamics of the remaining, mobile particles to increasingly slow down relative to the unconfined bulk liquid. Figure 4 shows new results on random pinning in a Kob-Andersen Lennard-Jones mixture (N = 5000 particles), at three pairs of state points, each pair chosen to share the same bulk τ_α. The α relaxation time increases with increasing pinning fraction (decreasing confining length L), and for state points with higher bulk τ_α, the decrease begins at a larger L reflecting a larger value of ξ. For state points with the same bulk τ_α, the dependence of τ_α on confining length is identical, and therefore ξ is constant at constant τ_α.

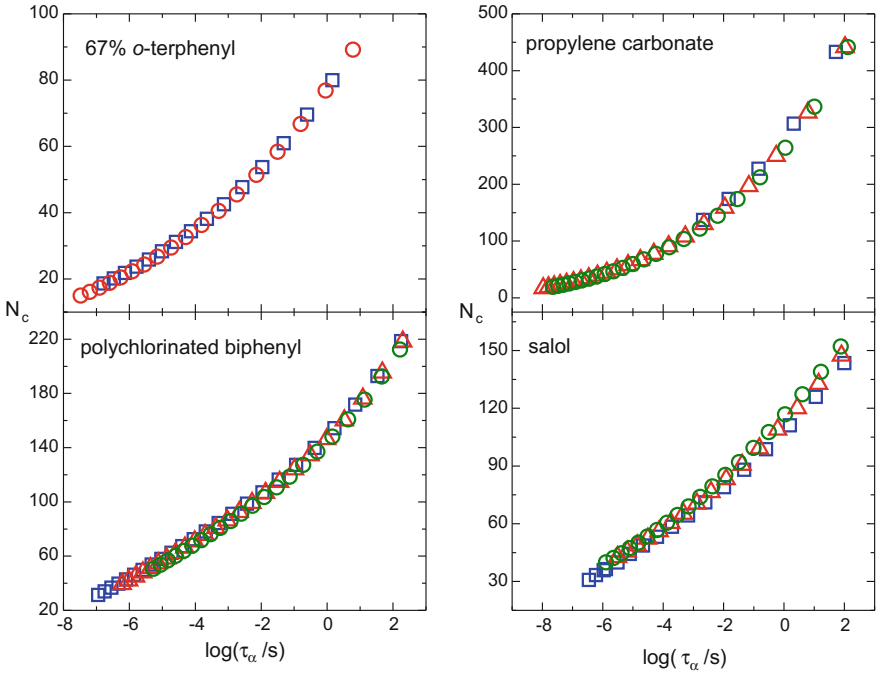

Fig. 5 Constancy of isochronal N_c calculated using Eq. (6) for four liquids. Adapted from Ref. [51]

The merging of the segmental and normal modes in polyisoprene measured at various pressures corresponded to fixed τ_α [32]. If the dynamic correlation volume is equal to the chain coil size at the state point associated with the merging, this result is consistent with constant N_c at fixed τ_α, since the change in the chain radius of gyration with T and P is small (<0.3% based on the measured dielectric strength of the normal mode) [32].

An analysis was carried out on four molecular liquids for which τ_α had been measured as a function of temperature and pressure [57]. As shown in Fig. 5, for a given material, the dynamic correlation volume, evaluated using the approximate Eq. (6), depends on the relaxation time, invariant to T, P, and ρ at fixed τ_α. However, the results in Fig. 5 are at odds with two other studies. Koperwas et al. [54] analyzed dielectric data for three liquids using Eq. (6), and determined that the isochronal N_c for each decreases by as much as 50% for pressures up to a couple hundred MPa. Results for phenylphthalein dimethylether are shown in Fig. 2. Diametrically opposite results were reported by Alba-Simionesco et al. [58], who found that N_c for dibutyl phthalate increased with pressure at constant $\tau_\alpha = 1$ s (Fig. 6). Thus, from measurements on eight liquids, it was concluded that N_c is constant [51], increases [49], or decreases [52] with increasing pressure at constant τ_α. The disparate results of these three studies are not because the behavior of different materials can qualitatively

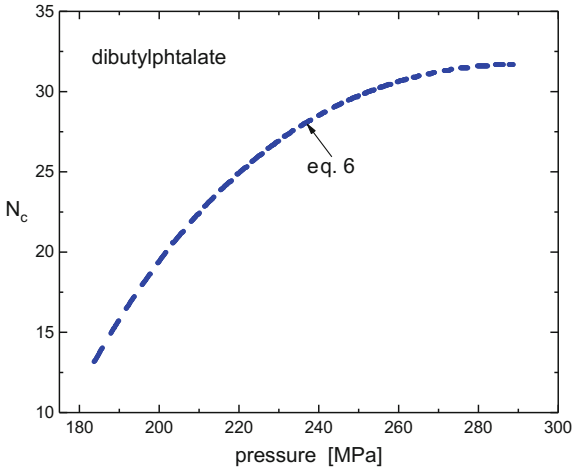

Fig. 6 Number of dynamically correlated molecules calculated using the indicated approximation [52]

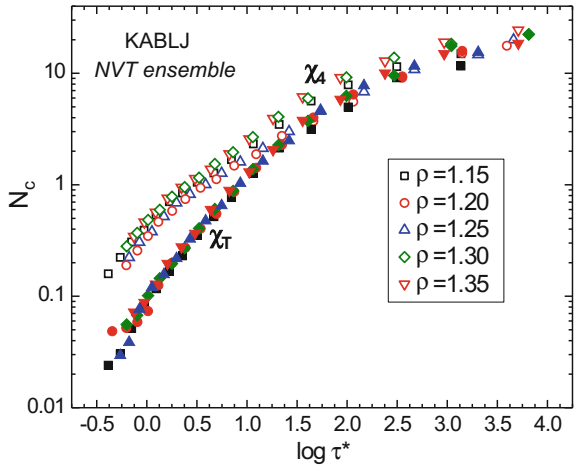

Fig. 7 Number of dynamically correlated particles calculated using Eq. (5) (open symbols) and Eq. (6) (solid symbols) at the indicated densities. From data in [9]

differ, but rather such results cast aspersions on the analysis using the approximate formula for $\chi_4(t)$.

One way to circumvent the ambiguity and inaccuracies in the application of Eqs. (6) and (8) is to obtain the full $\chi_4(t)$, which is possible using computer simulations. It is more convenient to calculate this multipoint dynamic susceptibility as the variance of the self-intermediate scattering function $F_s(k, t)$

$$\chi_4 = N_A \left[\left\langle f_s^2(k,t) \right\rangle - F_s^2(k,t) \right] \tag{9}$$

where $f_s(k, t)$ is the instantaneous value such that $\langle f_s(k, t) \rangle = F_s(k, t)$. Results are shown for a binary LJ liquid calculated in the NVT ensemble [which omits the second term on the rhs of Eq. (7)] in Fig. 7 [9]. The dynamic correlation volume is to

good approximation invariant at fixed α-relaxation time. Likewise, MD simulations of diatomic molecules indicated constant isochronal N_c (4% variation in the NVT ensemble; 8% in the NPT) [59].

4 Isochronal N_c from Nonlinear Dielectric Susceptibility

From both MD simulations [9, 51, 53] and the application of approximations to estimate $\chi_4(t)$ from experimental data [19, 32, 50], the conclusion seems to be that N_c is constant for fixed τ_α, independent of T, P, or ρ. However, there are scattered results to the contrary [49, 52], and the reliability of the estimates of N_c might be questioned. Accordingly, an alternative method is desirable.

Bouchaud and Biroli [60] proposed that the nonlinear dielectric susceptibility can be used to measure dynamic correlations in glassforming liquids, specifically that the peak height of the nonlinear susceptibility of glassforming materials increases in proportion to N_c:

$$N_c \propto |\chi_3| \frac{kT}{\varepsilon_0 a^3 (\Delta\chi_1)^2} \tag{10}$$

where ε_0 is the permittivity of free space, a is the molecular volume, $\Delta\chi_1$ is the linear dielectric strength, and $|\chi_3|$ is the modulus of the third-order susceptibility corresponding to polarization cubic in the applied field. The connection between χ_3 and N_c is supported by good agreement of the calculated N_c with the effective activation energy in glassforming liquids [61, 62], and plastic crystals [63]:

$$\left.\frac{\mathrm{d}\ln\tau}{\mathrm{d}T^{-1}}\right|_P = AN_c \tag{11}$$

where A is a constant. This analysis has also been extended to the fifth-order susceptibility χ_5, and results consistent with this analysis are obtained for glycerol and propylene carbonate [64]. The derivation of Eq. (10) is not rigorous, and growing nonlinear susceptibility with similar features to those observed experimentally also appear in mean-field models that lack length scales [65, 66]. An alternative phenomenological model of nonlinear dielectric response that lacks dynamic correlations also produces a growth of the peak in χ_3 proportionally to the apparent activation energy [67, 68]. It is not clear whether these different pictures of nonlinear relaxation are in conflict: based on a careful analysis of the behavior of the three different third-order susceptibilities, it has been suggested that in fact the models of Refs. [67, 68] are consistent with the interpretation leading to Eq. (10), i.e., relating the growth of χ_3 to the growth of cooperatively rearranging regions [69].

Equation (10) provides a method of testing whether N_c is constant under isochronal conditions, by measuring the third-order dielectric susceptibility at ele-

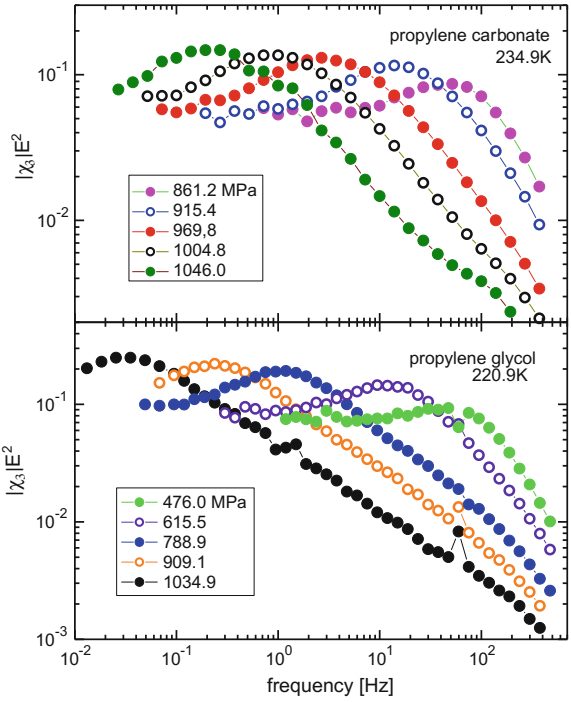

Fig. 8 Representative third-order harmonic spectra of propylene carbonate (top) and propylene glycol (bottom) at the indicated temperature and pressures, the latter increasing from right to left. From Ref. [59]

vated pressures. This was done for two liquids: propylene carbonate and propylene glycol [59].

Propylene carbonate is a non-associated liquid, conforming to isochronal superposition, meaning that its relaxation spectrum is constant for constant relaxation time. For the hydrogen-bonded propylene glycol, the relaxation spectrum becomes broader at for higher pressure and temperature at constant τ. Figure 8 presents $|\chi_3|$ spectra obtained at various pressures. For both liquids, the peak in nonlinear susceptibility grows with decrease in peak frequency, consistent with growth in the correlation volume as the relaxation time becomes longer.

To quantify the dynamic correlations, it is required that the contribution to $|\chi_3|$ from saturation of the dipole orientation be removed from the spectra; this was done following Brun et al. [70] who have shown that $|\chi_3|$ at a frequency 2.5 times the frequency of the maximum in the linear dielectric loss provides a measure of N_c unaffected by dipole saturation. In Fig. 9, N_c for the two liquids are plotted as a function of the linear relaxation frequency. The data for propylene carbonate show the two regimes expected for dynamic correlations—power-law dependences with a steeper slope at higher frequencies [71]. This supports the interpretation of the

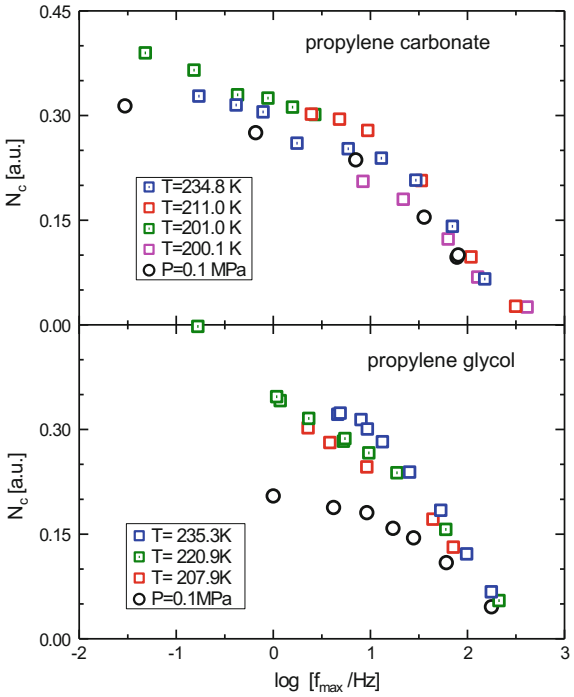

Fig. 9 Number of dynamically correlated molecules (arbitrary units) calculated using Eq. (10) for propylene carbonate (top) and propylene glycol (bottom) as a function of the frequency of the loss peak in the linear spectrum. From Ref. [59]

peak in the nonlinear susceptibility in terms of dynamic correlations. Within the experimental scatter (*ca.* 15%), the number of dynamically correlated molecules for propylene carbonate depends mainly on the relaxation time; there is no systematic variation in N_c with T or P. For propylene glycol, the large concentration of hydrogen bonds changes with thermodynamic conditions, resulting in liquid structure which is not constant at constant τ; indeed, the variety of scaling properties found for simple liquids are absent in associated materials [72]. This is also reflected in substantial variations (exceeding 50%) in N_c for a given τ, specifically a systematic increase in dynamic correlations with increasing temperature or pressure at constant τ.

When high pressures are considered, the values of N_c deviate from the proportionality with effective activation energy which holds at ambient pressure (Fig. 10). Thus, the parameter A in Eq. 10 is pressure dependent. For the case of non-associated liquids such as propylene carbonate, which conform to density scaling, it can be shown that the apparent activation energy is not a constant at constant τ [59]. Since N_c *is* constant (to good approximation), the deviation from strict proportionality of the two quantities can be understood. For associated liquids such as propylene glycol, the decoupling is stronger, additionally reflecting the change in structure at constant τ.

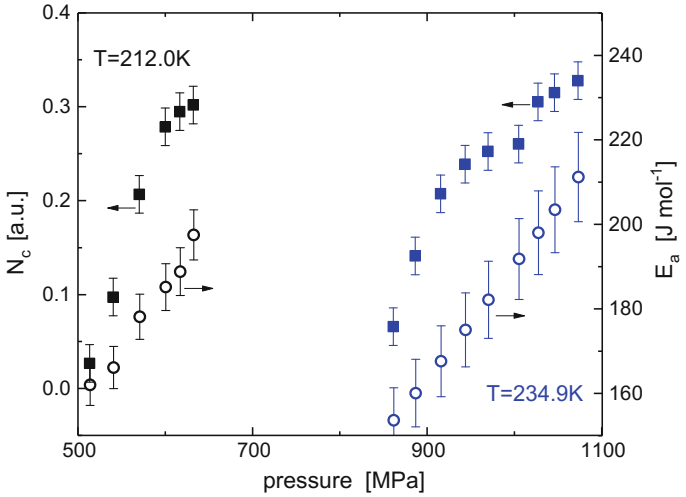

Fig. 10 Comparison of the temperature dependence of the number of dynamically correlated molecules calculated using Eq. (10) (filled squares) and the apparent activation energy (open circles) for propylene carbonate at the indicated temperatures. From Ref. [59]

5 Summary

Approximate analyses of experimental data and molecular dynamic simulations, which of course entail inherent approximations, indicate that ξ and N_c are constant under isochronal conditions. Such results are consistent with nonlinear dielectric measurements interpreting the modulus of the susceptibility as a measure of the dynamic correlation volume. This consistency supports the interpretation of the nonlinear response in terms of dynamic correlation, but more importantly establishes the centrality of dynamic heterogeneity to the glass transition phenomenon.

Acknowledgements This work was supported by the Office of Naval Research.

References

1. B. Frick, C. Alba-Simionesco, K.H. Andersen, L. Willner, Influence of density and temperature on the microscopic structure and the segmental relaxation of polybutadiene. Phys. Rev. E **67**, 051801 (2003)
2. A. Cailliaux, C. Alba-Simionesco, B. Frick, L. Willner, I. Goncharenko, Phys. Rev. E **67**, 010802 (2003)
3. R. Bohmer, Nanoscale heterogeneity of glass-forming liquids: experimental advances. Cur. Opin. Sol. State Mat. Sci. **3**, 378–385 (1998)
4. H. Sillescu, Heterogeneity at the glass transition: a review. J. Non-Cryst. Solids **243**, 81–108 (1999)

5. M.D. Ediger, Spatially heterogeneous dynamics in supercooled liquids. Ann. Rev. Phys. Chem. **51**, 99–128 (2000)
6. H. Sillescu, R. Bohmer, G. Diezemann, G. Hinze, Heterogeneity at the glass transition: what do we know? J. Non-Cryst. Sol. **307–310**, 16–23 (2002)
7. R. Richert, N. Israeloff, C. Alba-Simionesco, F. Ladieu, D. L'Hote, *Experimental approaches to heterogeneous dynamics* in Dynamical Heterogeneities in Glasses, Colloids, and Granular Media, ed. by L. Berthier, G. Biroli, J.-P. Bouchaud, L. Cipelletti, W. van Saarloos (Oxford University Press, Oxford, 2011)
8. K. Kim, S. Saito, Multiple length and time scales of dynamic heterogeneities in model glass-forming liquids: a systematic analysis of multi-point and multi-time correlations. J. Chem. Phys. **138**, 12A506 (2013)
9. C.M. Roland, D. Fragiadakis, D. Coslovich, S. Capaccioli, K.L. Ngai, Correlation of nonexponentiality with dynamic heterogeneity from four-point dynamic susceptibility $\chi_4(t)$ and its approximation $\chi_T(t)$. J. Chem. Phys. **133**, 124507 (2010)
10. R. Böhmer, K.L. Ngai, C.A. Angell, D.J. Plazek, Nonexponential relaxations in strong and fragile glass formers. J. Chem. Phys. **99**, 4201–4209 (1993)
11. K. Niss, C. Dalle-Ferrier, G. Tarjus, C. Alba-Simionesco, On the correlation between fragility and stretching in glass-forming liquids. J. Phys. Cond. Mat. **19**, 076102 (2007)
12. E.R. Weeks, J.C. Crocker, A.C. Levitt, A. Schofield, D.A. Weitz, Three-dimensional direct imaging of structural relaxation near the colloidal glass transition. Science **287**, 627–631 (2000)
13. O. Dauchot, G. Marty, G. Biroli, Dynamical heterogeneity close to the jamming transition in a sheared granular material. Phys. Rev. Lett. **95**, 265701 (2005)
14. G. Adam, J.H. Gibbs, On the temperature dependence of cooperative relaxation properties in glass-forming liquids. J. Chem. Phys. **43**, 139–146 (1965)
15. K.S. Schweizer, E.J. Saltzman, Activated hopping, barrier fluctuations, and heterogeneity in glassy suspensions and liquids. J. Phys. Chem. B **108**, 19729–19741 (2004)
16. J.P. Garrahan, D. Chandler, Dynamics on the way to forming glass: bubbles in space-time. Ann. Rev. Phys. Chem. **61**, 191–217 (2010)
17. V. Lubchenko, P.G. Wolynes, Theory of structural glasses and supercooled liquids. Ann. Rev. Phys. Chem. **58**, 235–266 (2007)
18. A. Heuer, Exploring the potential energy landscape of glass-forming systems: from inherent structures via metabasins to macroscopic transport. J. Phys. Con. Mat. **20**, 373101 (2008)
19. F. Rittig, A. Huwe, G. Fleischer, J. Kärger, F. Kremer, Molecular dynamics of glass-forming liquids in confining geometries. Phys. Chem. Chem. Phys. **1**, 519–523 (1999)
20. G. Dosseh, C. Le Quellec, N. Brodie-Lindner, C. Alba-Simionesco, W. Haeussler, P. Levitz, Fluid–wall interactions effects on the dynamical properties of confined orthoterphenyl. J. Non-Cryst. Sol. **352**, 4964–4968 (2006)
21. J. Koppensteiner, W. Schranz, M.A. Carpenter, Revealing the pure confinement effect in glass-forming liquids by dynamic mechanical analysis. Phys. Rev. B **81**, 024202 (2010)
22. C.L. Jackson, G.B. McKenna, The glass transition of organic liquids confined to small pores. J. Non-Cryst. Sol. **131–133**, 221–224 (1991)
23. Y.B. Melnichenko, J. Schuller, R. Richert, B. Ewen, C.K. Loong, Dynamics of hydrogen bonded liquids confined to mesopores—a dielectric and neutron spectroscopy study. J. Chem. Phys. **103**, 2016–2024 (1995)
24. F. Kremer, A. Huwe, M. Arndt, P. Behrens, W. Schwieger, How many molecules form a liquid? J. Phys. Cond. Mat. **11**, A175–A188 (1999)
25. A. Schonhals, H. Goering, C. Schick, B. Frick, R. Zorn, Glassy dynamics of polymers confined to nanoporous glasses revealed by relaxational and scattering experiments. Eur. Phys. J. E **12**, 173–178 (2003)
26. A. Schonhals, H. Goering, C. Schick, B. Frick, M. Mayorova, R. Zorn, Segmental dynamics of poly(methyl phenyl siloxane) confined to nanoporous glasses. Eur. Phys. J. Spec. Topics. **141**, 255–259 (2007)
27. J.P. Bouchaud, G. Biroli, On the Adam-Gibbs-Kirkpatrick-Thirumalai-Wolynes scenario for the viscosity increase in glasses. J. Chem. Phys. **121**, 7347–7354 (2004)

28. G. Biroli, J.-P. Bouchaud, A. Cavagna, T.S. Grigera, P. Verrocchio, Thermodynamic signature of growing amorphous order in glass-forming liquids. Nat. Phys. **4**, 771–775 (2008)
29. S. Yaida, L. Berthier, P. Charbonneau, G. Tarjus, Point-to-set lengths, local structure, and glassiness. Phys. Rev. E **94**, 032605 (2016)
30. W. Kob, S. Roldán-Vargas, L. Berthier, Non-monotonic temperature evolution of dynamic correlations in glass-forming liquids. Nat. Phys. **8**, 164 (2012)
31. G.M. Hocky, L. Berthier, W. Kob, D.R. Reichman, Static point-to-set correlations in glass-forming liquids. Phys. Rev. E **85**, 011102 (2012)
32. K. Hima Nagamanasa, S. Gokhale, A.K. Sood, R. Ganapathy, Direct measurements of growing amorphous order and non-monotonic dynamic correlations in a colloidal glass-former. Nat. Phys. **11**, 403 (2015)
33. S, Gokhale, K. Hima Nagamanasa, R. Ganapathy, A. K. Sood, Growing dynamic facilitation on approaching the random pinning colloidal glass transition. Nat. Commun. **5**, 4685 (2014)
34. B. Mei, Y. Lu, L. An, H. Li, L. Wang, Nonmonotonic dynamic correlations in quasi-tow-dimensional confined glass-forming liquids. Phys. Rev. E **95**, 050601(R) (2017)
35. A. Schonhals, E. Schlosser, Relationship between segmental and chain dynamics in polymer melts as studied by dielectric spectroscopy. Phys. Scr. **T49**, 233–236 (1993)
36. C. Gainaru, W. Hiller, R. Bohmer, A dielectric study of oligo- and poly(propylene glycol). Macromolecules **43**, 1907–1914 (2010)
37. D. Fragiadakis, R. Casalini, R.B. Bogoslovov, C.G. Robertson, C.M. Roland, Dynamic heterogeneity and density scaling in 1,4-polyisoprene. Macromolecules **44**, 1149–1155 (2011)
38. U. Tracht, M. Wilhelm, A. Heuer, H. Feng, K. Schmidt-Rohr, H.W. Spiess, Length scale of dynamic heterogeneities at the glass transition determined by multidimensional nuclear magnetic resonance. Phys. Rev. Lett. **81**, 2727–2730 (1998)
39. S.A. Reinsberg, X.H. Qiu, M. Wilhelm, H.W. Spiess, M.D. Ediger, Length scale of dynamic heterogeneity in supercooled glycerol near T_g. J. Chem. Phys. **114**, 7299–7302 (2001)
40. S.A. Reinsberg, A. Heuer, B. Doliwa, H. Zimmermann, H.W. Spiess, Comparative study of the NMR length scale of dynamic heterogeneities of three different glass formers. J. Non-Cryst. Solid **307–310**, 208–214 (2002)
41. X.H. Qiu, M.D. Ediger, Length scale of dynamic heterogeneity in supercooled d-sorbitol: comparison to model predictions. J. Phys. Chem. B **107**, 459–464 (2003)
42. E. Donth, The size of cooperatively rearranging regions at the glass transition. J. Non-Cryst. Sol. **53**, 325–330 (1982)
43. K. Schroter, Characteristic length of glass transition heterogeneity from calorimetry. J Non-Cryst. Sol. **352**, 3249–3254 (2006)
44. A. Saiter, L. Delbreilh, H. Couderc, K. Arabeche, A. Schönhals, J.-M. Saiter, Temperature dependence of the characteristic length scale for glassy dynamics: Combination of dielectric and specific heat spectroscopy. Phys. Rev. E **81**, 041805 (2010)
45. E. Hempel, G. Hempel, A. Hensel, C. Schick, E. Donth, Characteristic length of dynamic glass transition near t_g for a wide assortment of glass-forming substances. J. Phys. Chem. B **104**, 2460–2466 (2000)
46. C. Dasgupta, A.V. Indrani, S. Ramaswamy, M.K. Phani, Is there a growing correlation length near the glass transition? Europhys. Lett. **15**, 307–312 (1991)
47. L. Berthier, G. Biroli, Theoretical perspective on the glass transition and amorphous materials. Rev. Mod. Phys. **83**, 587–645 (2011)
48. L. Berthier, G. Biroli, J.-P. Bouchaud, L. Cipelletti, D. El Masri, D. L'Hote, F. Ladieu, M. Pierno, Direct experimental evidence of a growing length scale accompanying the glass transition. Science **310**, 1797–1800 (2005)
49. C. Dalle-Ferrier, C. Thibierge, C. Alba-Simionesco, L. Berthier, G. Biroli, J.P. Bouchaud, F. Ladieu, D. L'Hote, G. Tarjus, Spatial correlations in the dynamics of glassforming liquids: experimental determination of their temperature dependence. Phys. Rev. E **76**, 041510 (2007)
50. L. Berthier, G. Biroli, J.-P. Bouchaud, L. Cipelletti, D. El Masri, D. L'Hôte, F. Ladieu, M. Pierno, Direct experimental evidence of a growing length scale accompanying the glass transition. Science **310**, 1797–1800 (2005)

51. L. Berthier, G. Biroli, J.-P. Bouchaud, W. Kob, K. Miyazaki, D.R. Reichman, Spontaneous and induced dynamic fluctuations in glass formers. 1. General results and dependence on ensemble and dynamics. J. Chem. Phys. **126**, 184503 (2007)
52. S. Capaccioli, G. Ruocco, F. Zamponi, Dynamically correlated regions and configurational entropy in supercooled liquids. J. Phys. Chem. B **112**, 10652–10658 (2008)
53. E. Flenner, G. Szamel, Dynamic heterogeneities above and below the mode-coupling temperature: evidence of a dynamic crossover. J. Chem. Phys. **138**, 12A523 (2013)
54. K. Koperwas, A. Grzybowski, K. Grzybowska, Z. Wojnarowska, A.P. Sokolov, M. Paluch, Effect of temperature and density fluctuations on the spatially heterogeneous dynamics of glass-forming van der Waals liquids under high pressure. Phys. Rev. Lett. **111**, 125701 (2013)
55. R. Casalini, L. Zhu, E. Baer, C.M. Roland, Segmental dynamics and the correlation length in nanoconfined PMMA. Polymer **88**, 133–136 (2016)
56. T.S. Ingebrigtsen, J.R. Errington, T.M. Truskett, J.C. Dyre, Predicting how nanoconfinement changes the relaxation time of a supercooled liquid. Phys. Rev. Lett. **111**, 235901 (2013)
57. D. Fragiadakis, R. Casalini, C.M. Roland, Density scaling and dynamic correlations in viscous liquids. J. Phys. Chem. B **113**, 13134–13147 (2009)
58. C. Alba-Simionesco, C. Dalle-Ferrier, G. Tarjus, Effect of pressure on the number of dynamically correlated molecules when approaching the glass transition. AIP Conf. Proc. **1518**, 527–535 (2013)
59. R. Casalini, D. Fragiadakis, C.M. Roland, Dynamic correlation length scales under isochronal conditions. J. Chem. Phys. **142**, 064504 (2015)
60. J.-P. Bouchaud, G. Biroli, Nonlinear susceptibility in glassy systems: a probe for cooperative dynamical length scales. Phys. Rev. B **72**, 064204 (2005)
61. C. Crauste-Thibierge, C. Brun, F. Ladieu, D. L'Hôte, G. Biroli, J.-P. Bouchaud, Evidence of growing spatial correlations at the glass transition from nonlinear response experiments. Phys. Rev. Lett. **104**, 165703 (2010)
62. Th Bauer, P. Lunkenheimer, A. Loidl, Cooperativity and the freezing of molecular motion at the glass transition. Phys. Rev. Lett. **111**, 225702 (2013)
63. M. Michl, Th Bauer, P. Lunkenheimer, A. Loidl, Nonlinear dielectric spectroscopy in a fragile plastic crystal. J. Chem. Phys. **144**, 114506 (2016)
64. S. Albert, Th Bauer, M. Michl, G. Biroli, J.-P. Bouchaud, A. Loidl, P. Lunkenheimer, R. Tourbot, C. Wiertel-Gasquet, F. Ladieu, Fifth-order susceptibility unveils growth of thermodynamic amorphous order in glass-formers. Science **352**, 1308 (2016)
65. G. Diezemann, Higher-order correlation functions and nonlinear response functions in a Gaussian trap model. J. Chem. Phys. **138**, 12A505 (2013)
66. C. Brun, C. Crauste-Thibierge, F. Ladieu, D. L'Hôte, Third harmonics nonlinear susceptibility in supercooled liquids: a comparison to the box model. J. Chem. Phys. **134**, 194507 (2011)
67. P. Kim, A.R. Young-Gonzales, R. Richert, Dynamics of glass-forming liquids. XX. Third harmonic experiments of non-linear dielectric effects versus a phenomenological model. J. Chem. Phys. **145**, 064510 (2016)
68. R. Richert, Nonlinear dielectric signatures of entropy changes in liquids subject to time dependent electric fields. J. Chem. Phys. **144**, 114501 (2016)
69. P. Gadige, S. Albert, M. Michl, Th Bauer, P. Lunkenheimer, A. Loidl, R. Tourbot, C. Wiertel-Gasquet, G. Biroli, J.-P. Bouchaud, F. Ladieu, Unifying different interpretations of the nonlinear response in glass-forming liquids. Phys. Rev. E **96**, 032611 (2017)
70. C. Brun, F. Ladieu, D. L'Hôte, M. Tarzia, G. Biroli, J.-P. Bouchaud, Nonlinear dielectric susceptibilities: accurate determination of the growing correlation volume in a supercooled liquid. Phys. Rev. B **84**, 104204 (2011)
71. Dynamical Heterogeneities in Glasses, Colloids and Granular Materials, ed. by L. Berthier, G. Biroli, J.-P. Bouchaud, L. Cipelletti, W. van Saarloos (Oxford University Press, Oxford, 2011)
72. C.M. Roland, R. Casalini, R. Bergman, J. Mattsson, Role of hydrogen bonds in the supercooled dynamics of glass-forming liquids at high pressures. Phys. Rev. B **77**, 012201 (2008)